A reliable indicator to detect non-adjacent broken rotor bars severity in induction motors

Gyftakis, K. , Antonino-Daviu, J. A. and Marques Cardoso, A. J.

Original citation & hyperlink:
Gyftakis, K. , Antonino-Daviu, J. A. and Marques Cardoso, A. J. (2016) 'A Reliable Indicator to Detect Non-Adjacent Broken Rotor Bars Severity in Induction Motors' In: IEEE Transactions on Industry Applications, 'XXIIth International Conference on Electrical Machines (ICEM'2016)'. Held 4-7 September 2016 at Lausanne, Switzerland. IEEE, 2910 - 2916.
http://dx.doi.org/10.1109/ICELMACH.2016.7732937

DOI 10.1109/ICELMACH.2016.7732937
ISBN 978-1-5090-2538-1
ISBN 978-1-5090-2537-4
ISBN 978-1-5090-2539-8

Publisher: IEEE

A Reliable Indicator to Detect Non-Adjacent Broken Rotor Bars Severity in Induction Motors

K. N. Gyftakis, J. A. Antonino-Daviu and A. J. Marques Cardoso

Abstract – **The reliable diagnostic of non-adjacent rotor bar breakages in induction motors based on the analysis of currents is still an unsolved industrial problem. The traditional MCSA has not proven to be robust enough for assessing the rotor condition under this situation; this is due to the fact that the joint effect of breakages located at certain relative positions can be subtractive rather than additive, leading to decrements in the fault harmonics amplitudes rather than incrementing them. This work takes advantage of the potential of the novel Filtered Park's/Extended Park's Vector Approach (FPVA/FEPVA); this method has proven to overcome some constraints of the traditional Park's Vector-based methods: in this work, it is proven how this method can also reliably assess the rotor condition even if non-adjacent breakages are present. The user-friendly results obtained with the method confer it a great potential for its future implementation in autonomous fault diagnosis devices.**

***Index Terms*—Induction Motors, Fault Diagnosis, Broken Rotor Bars, Park's Vector.**

I. Introduction

INDUCTION motors are the most widespread rotating electrical machines in industry. They are considered as the 'workhorses' of the industrial sector by many authors [1]. Although cage induction motors are very reliable machines, they are prone to suffer several types of failures as stator insulation faults, bearing damages, rotor failures, core defects, etc. The extensive utilization of these machines justifies the development of reliable techniques for the detection of these possible failures, even when these faults are in their early stages of development.

Rotor cage damages account for less than 20% of the possible faults in induction motors [1], [2]. However, this type of fault is more common in large motors that operate under heavy duty cycles and that start under high-inertias. These are, indeed, the most critical machines and those with a most difficult and expensive repair [3], [4]. On the other hand, despite in most cases rotor damages require relatively long times to develop, so that the machine can still operate although the fault is present, some cases of catastrophic effects of this failure have been also reported [3], [5]. In these situations, the consequences of the forced outage of the machine have been very serious: huge economic losses, production downtimes, repair times, user safety hazard, etc. These factors have justified the great effort spent in the development of techniques for reliably diagnosing this type of faults.

Traditionally, methods based on analysis of currents have been employed to assess the rotor condition of induction motors. The traditional method, known as Motor Current Signature Analysis (MCSA), is based on capturing the current demanded by the machine during steady-state operation and on the further application of the FFT to evaluate the amplitudes of different families of components that are amplified by the fault [1], [6], [7]. The most relevant of these components are the well-known sideband harmonics with frequencies given by $f\cdot(1\pm2\cdot s)$ (f=supply frequency and s=slip) [1]. Despite MCSA has provided satisfactory results when assessing the rotor health over years, it also has serious disadvantages. One of these drawbacks is the fact that it can lead to eventual false indications (either positive or negative) in many situations that, on the other hand, may be rather common in industry. In this regard, recent works have reported possible false indications of MCSA in the case of presence of pulsating load torques [8], [9], existence of rotor cooling ducts [4] or magnetic core anisotropy [10], diagnosis under low-slip conditions [9] or presence of broken outer bars in double cage rotors [11], among others. In these situations, alternative approaches such as the analysis of the power signature [12], [13], motor startup current [4], [9], [11], the application of the modified Prony method [14], or off-line methods [10], [15] have been proposed to overcome the MCSA problems, showing very high potential.

One of the cases where the application of MCSA has frequently led to false negative indications is the presence of non-adjacent broken bars in the rotor cage. In previous works it was proven that when two bars are broken in the rotor cage, if their position is non-adjacent, their effects can partially compensate [16]; this is, rather than leading to an increase in the amplitude of the sideband harmonics, in comparison with the one-broken bar situation, the joint effect of the two broken bars can be a reduced sideband that can be even comparable to the amplitude under healthy conditions [16]. This situation was deeply studied and theoretically justified by many authors: in [17], [18], the difficulties of current analysis for detecting bars fractured at intervals of $\pi/2$ electrical radians were already pointed out. Other works as [19] proved that the

This work was supported in part by the Spanish 'Ministerio de Economía y Competitividad' (MINECO) and FEDER program in the framework of the 'Proyectos I+D del Subprograma de Generación de Conocimiento, Programa Estatal de Fomento de la Investigación Científica y Técnica de Excelencia' (ref: DPI2014-52842-P)."

K. N. Gyftakis is with the School of CEM, Faculty of EEC and with the Research Centre for Mobility and Transport, Coventry University, Priory St, Coventry, UK, CV15FB (e-mail: k.n.gyftakis@ieee.org).

J. A. Antonino-Daviu is with the Instituto Tecnologico de la Energia, Universitat Politècnica de València, Camino de Vera s/n, 46022, Valencia, Spain (e-mail: joanda@die.upv.es).

A. J. M. Cardoso is with CISE – Electromechatronic Systems Research Centre, Universidade da Beira Interior, P – 6201-001 Covilhã, Portugal (e-mail: ajmcardoso@ieee.org).

amplitude of the lower sideband harmonic strongly varies with the relative position between the broken bars; this work stated that for certain positions, the effect of two breakages can be lower than that of a single breakage. [20], [21] also dealt with this issue by developing models where the case of non-adjacent breakages is taken into consideration. In [22] a thorough study of the induction motor with non-adjacent broken bars is carried out. Finally, in [16] a physical analysis of the air-gap magnetic anomaly for the case of any double bar breakage is performed. In that paper, simple expressions for the approximate calculation of the lower sideband amplitude as a function of the relative position of the broken bars are deduced.

Though some approaches with certain promising potential have been proposed to overcome this situation [23], up to now, no method has been proven to be enough reliable to detect and evaluate the severity of the aforementioned fault.

In this paper, the authors propose the application of a procedure based on the Filtered Park's and Filtered Extended Park's Vector Approach (FPVA and FEPVA, respectively) to reliably diagnose broken rotor bars fault in induction motors, even when these are non-adjacent. The method relies on the monitoring of higher harmonic index of the Park's vector. The work relies on experimental data and the results prove the method's effectiveness and reliability. Moreover, unlike other techniques, this method provides a completely user friendly output that enables to clearly identify the fault condition, even by non-expert users. This confers a great potential for the future implementation of the method in real industrial systems as well as for facilitating the automation of the diagnosis process, which is a crucial aspect for implementation in portable condition monitoring devices.

II. THE FPVA AND FEPVA PROCEDURE

The traditional PVA [24], as well as later methods derived on it [25], rely on the monitoring of the three-phase or line currents of the IM namely: i_a, i_b, i_c.

The Park's Vector components, I_d and I_q, are then calculated by:

$$I_d = \left(\sqrt{2}/\sqrt{3}\right) i_a - \left(1/\sqrt{6}\right) i_b - \left(1/\sqrt{6}\right) i_c \tag{1}$$

$$I_q = \left(1/\sqrt{2}\right) i_b - \left(1/\sqrt{2}\right) i_c \tag{2}$$

Under ideal conditions, i. e. for a healthy three-phase IM, fed by a direct three-phase sinusoidal voltage supply system, the three phase currents lead to a Park's vector with the following components:

$$I_d = \left(\sqrt{6}/\sqrt{2}\right) I_M \sin(\omega t) \tag{3}$$

$$I_q = \left(\sqrt{6}/\sqrt{2}\right) I_M \sin(\omega t - \pi/2) \tag{4}$$

where:

I_M : maximum value of the supply phase current (A)

ω : angular supply frequency (rad/s)

t : time variable (s)

The corresponding representation of the Park's Vector is a circular locus centered at the origin of the coordinates. It is well known, that the occurrence of broken rotor bars will cause the appearance of a spectral component located at: $f_s - 2sf_s$ in the motor supply current spectrum. It was shown in the past that due to the speed ripple phenomenon another harmonic will also appear at: $f_s + 2sf_s$. The appearance of these harmonics in the current spectra will cause an increase of the Park's Vector ring thickness [26].

The above described technique is simplified due to the fact that it considers pure sinusoidal shape of the IM currents. In reality, each phase/line current i_{ph} contains the following terms for an ideal IM:

$$i_{ph} = i_{MMF} + i_{sat} + i_{RSH} \tag{5}$$

where:

$$i_{MMF} = \sum_{n=6k\pm1} i_n \cos(\omega_n t) \tag{6}$$

$$i_{sat} = \sum_{m=2l\pm1} i_m \cos(\omega_m t + \varphi_{sat}) \tag{7}$$

$$i_{RSH} = \sum_{u} i_u \left({N_R}/{p}\right)(u - s) f_s \tag{8}$$

N_R : rotor slot number, p: pole pairs number, s: slip, k,l,u: integers

i_{MMF} : Current harmonics produced by the stator winding configuration.

i_{sat} : Current harmonics due to iron core saturation.

i_{RSH} : Current harmonics due to the rotor slots.

In real induction motors more harmonics are expected to show. This is due to the fact that the manufacturing process can introduce certain asymmetries such as static and dynamic eccentricity, different resistance of windings, high resistance connections. Also, the supply is not ideal and this will also impact the harmonic index of the produced magnetic field.

Furthermore, the proposed strategy is the following: the three phase current waveforms are firstly monitored. This can be done via a simple and non-invasive way, provided that the access to the phase currents is available. The sampling frequency addopted in this work has been 5 kHz. The next step is to calculate the Park's Vector components. At this point, an elliptic filter is applied to cutoff frequencies greater than 270 Hz in both d and q current components. Afterwards, the fundamental component is filtered using a notch filter. The Filtered Park's Vector is then represented. This can be the first indication of the fault's existence from the operator point of view. Finally, the modulus of the Filtered Park's Vector is calculated and its spectrum is studied with the application of the FFT to determine the severity of the fault.

For the experimental testing, six identical 3-phase, 4-pole induction motors are used: one with healthy rotor cage, one with a broken rotor bar, one with two adjacent broken rotor bars and three more with different distances between the two broken rotor bars. The motor characteristics are shown in Table I whereas the test bench is illustrated in Fig. 1.

Moreover, the separate motor cases have been named as follows to improve clarity:

- h: healthy
- b1: one broken bar
- b1_2: two adjacent broken bars
- b1_3: two broken bars (first and third)
- b1_4: two broken bars (first and fourth)
- b1_5: two broken bars (first and fifth)
- b1_6: two broken bars (first and sixth)

TABLE I
INDUCTION MOTOR CHARACTERISTICS

Rated power	1.1 kW
Rated frequency	50 Hz
Rated voltage	230 V
Rated primary current	4.5 A
Rated speed	1410 rpm
Rated slip	0.06
Stator windings connection	Delta
Number of pole pairs	2
Number of rotor bars	28
Number of stator slots	36

Fig. 1. The experimental test bench.

III. FPVA REPRESENTATION RESULTS

Following the steps described in the previous paragraph, the results from the application of this method will be demonstrated here. Firstly, the three stator phase currents are monitored and then the d and q components are calculated. The frequency spectrum of the d current is shown in Fig. 2–a. Secondly, the elliptic filter is applied to cutoff frequencies higher than 270 Hz (Fig. 2–b). Then the notch filter is applied and the final spectrum of the d current is shown in Fig. 2-c. Similar is the process to create a filtered version of the q current component. The notch filter affects the amplitude of the harmonics close to the 5th current hrmonic but the impact is low. It can be seen in Fig. 2-c that finally the 7th harmonic has slightly greater amplitude than the 5th. However, this does not affect the generalization of the method since both 5th and 7th current harmonics produce a family of broken rotor bar signatures with significant amplitudes. This happens due to the less magnetic flux penetration in the rotor body by the 5th and 7th harmonic orders of the produced magnetic field.

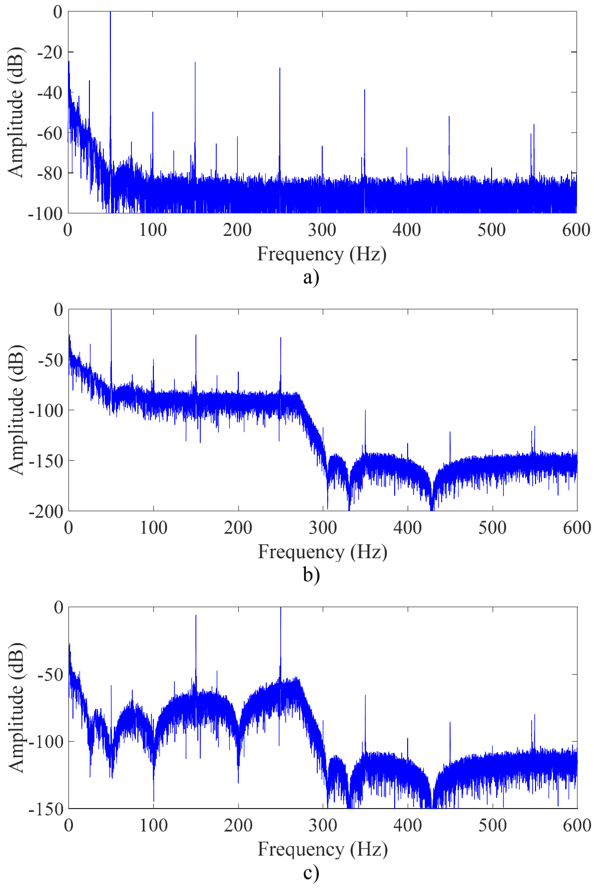

Fig. 2. Frequency spectra of the d current component of the Park's vector for the healthy induction motor: a) original signal, b) after the application of the elliptic filter and c) after the additional application of the notch filter.

The FPVA consists of the representation of the filtered d and q components of the Park's Vector. The occuring results are shown in Fig. 3 for all studied cases. The healthy motor has blue colour whereas all faulty cases have red. The lack of any broken bar fault related harmonics leads to a clear family of ellipses for the healthy induction motor case. If the motor was bigger, the width of the ellipsis would be even more concentrated. In this case the motor is small and thus more affected by strong inherent asymmetries. However, the representation agrees with the expectations.

In the faulty cases, it is now clear that the fault existence strongly affects the FPVA representation. The co-existence of the broken bar fault related sideband signatures next to the third and fifth harmonics, as well as the existence of the fundamental harmonic's broken bar fault related sidebands disturbs the symmetry of the FPVA representation. The ellipses can be seen in the case of one broken rotor bar fault case but they have started losing their concentration. Furthermore, all cases related to two broken bars (Fig3-c, d, e, f) result to configurations without the characteristic ellipses presence.

In a real industrial case, the visual inspection of a FPVA representation by non-expert personel can lead to a first reliable diagnostic alarm regarding broken bar fault existence.

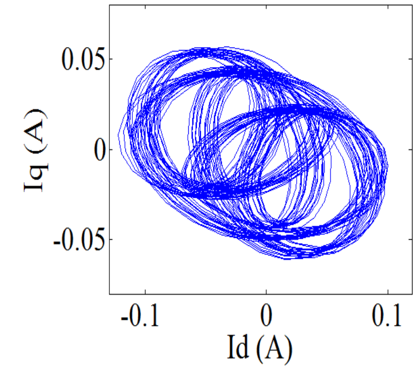

a)

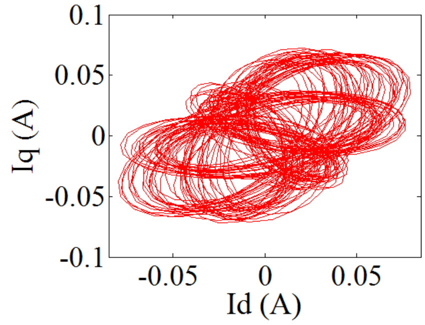

b)

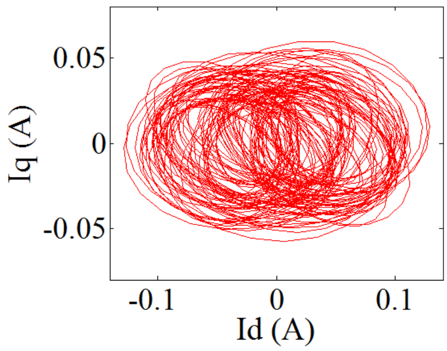

c)

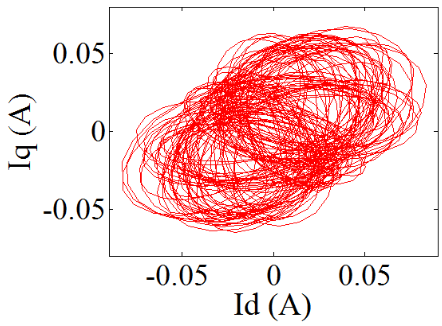

d)

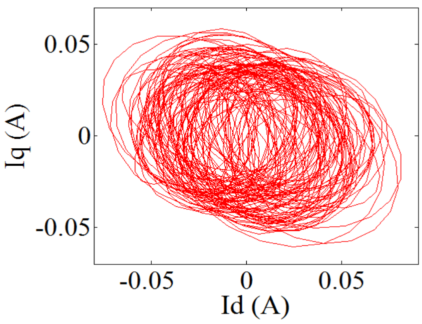

e)

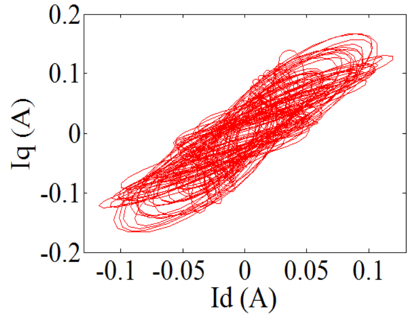

f)

Fig. 3. The FPVA pattern for the following induction motor cases: a) h, b) b1, c) b1_2, d) b1_3, e) b1_4 and f) b1_5.

After the visual confirmation of the fault's existence, a more thorough procedure will follow to determine with accuracy the broken rotor bar fault existence and severity. The next step of the proposed methodology is to calculate the Park's Vector Modulus using the filtered d and q components. Then the frequency spectra of the Park's Vector Modulus is calculated and studied. This is the FEPVA application step.

In Fig. 4 the results from the application of the FEPVA on all studied induction motor cases are illustrated. There is a variety of harmonics which increase with the fault existence. The FPV representation took into account the 5th and 7th higher harmonics of the current due to the strong broken bar fault signatures that are produced around them [28]-[29]. The existence of the above stator MMF produced current harmonics leads to the existence of a strong harmonic existing at $6f_s$ in the FPV modulus. More specifically, one can observe the increase of the components located at: $6f_s - 2ksf_s$, k=1,2,3,4,5 and $6f_s + 2nsf_s$, n=1,2. However, it is evident that the amplitude of each harmonic varies depending on the relative position between the two broken bars. Aiming for an improved insight, all harmonics amplitudes have been collected and presented in the upper part of Table II. Very strong variations were observed in the original data. This was caused by the amplitude difference of the $6f_s$ harmonic between the studied cases. This difference is caused by supply imbalances which are very strong due to the small size of the studied motors. However, to properly evaluate the findings all signatures have been normalized in each case by the $6f_s$ amplitude. The normalized data are shown in the lower part of Table II.

A closer look to the normalized data of Table II reveals that, none of the harmonics can stand on its own as a reliable fault level severity indicator. For example, the $6f_s - 10sf_s$ (1st column) has insignificant amplitude in the healthy motor. The increase of this harmonic is low for b1, b1_2 and b1_3 cases. Then it increases a lot for the b1_4 motor and drops a lot in the b1_5 one. Similar differences are observed using the other signatures. In some cases, it is difficult to discriminate the senario with one broken rotor bar from some senarios of two broken rotor bars. In the end, the impression is that a single signature is not reliable enough to detect the broken bar fault severity. This is not illogical since each one of the broken rotor bar fault related harmonics is produced by a different physical mechanism. For example, the interaction between the $3f_s$

main stator field and the sfs rotor field will lead to the well known $3f_s - 2sf_s$ and $3f_s - 4sf_s$ fault signatures. However, the $3f_s$ higher magnetic field will cause the production of the fault related $3f_s - 6sf_s$ harmonic, which will be more rotor saturation sensitive. The harmonics located to the right of the $6f_s$ are well known to be produced by the interaction of the broken bar fault and the speed ripple effect as it has been shown in the past in [27].

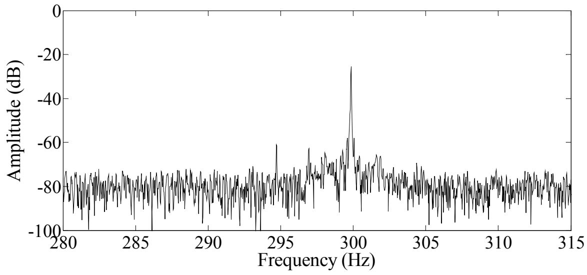

a)

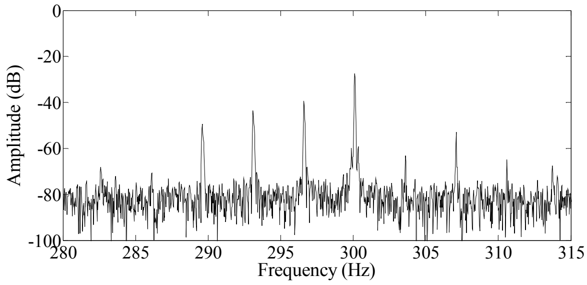

b)

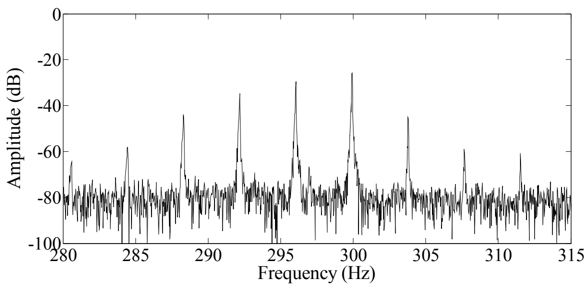

c)

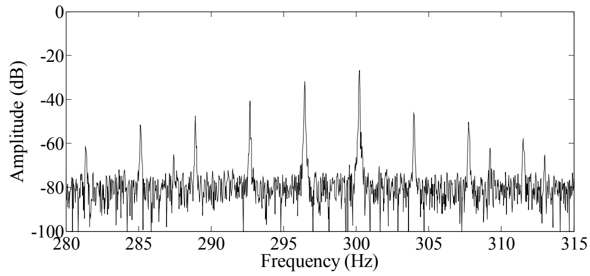

d)

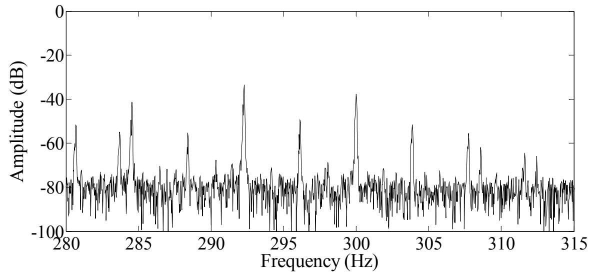

e)

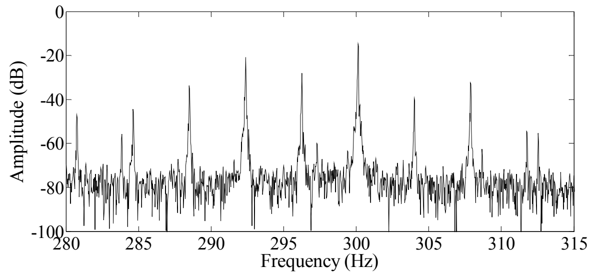

f)

Fig. 4. Application of the FEPVA. Frequency spectra of the FPV modulus for the cases: a) h, b) b1, c) b1_2, d) b1_3, e) b1_4 and f) b1_5.

Since single harmonics cannot reveal the non-adjacent broken bar fault severity, a different approach is adopted. A fault indicator is calculated, which is computed as the average of four signatures: $6f_s - 4sf_s$, $6f_s - 2sf_s$, $6f_s + 2sf_s$ and $6f_s + 4sf_s$. The above harmonics have been selected for the following reasons.

Firstly, the $6f_s - 4sf_s$ and $6f_s - 2sf_s$ are produced by the

TABLE II
BROKEN ROTOR BAR FAULT SIGNATURES AMPLITUDES FOR DIFFERENT INDUCTION MOTOR CASES AFTER APPLYING THE FEPVA

Motor case	**6·fs-10·s·fs**	**6·fs-8·s·fs**	**6·fs-6·s·fs**	**6·fs-4·s·fs**	**6·fs-2·s·fs**	**6·fs**	**6·fs+2·s·fs**	**6·fs+4·s·fs**	**6·fs+6·s·fs**
Original data									
Healthy	-72.23	-73.39	-73.34	-73.69	-62.84	-25.38	-71.38	-75.12	-73.06
b1	-68.14	-70.58	-49.39	-43.63	-39.4	-27.46	-63.2	-52.94	-64.83
b1_2	-64.34	-58.25	-43.92	-34.75	-29.59	-25.86	-45.1	-59.08	-60.09
b1_3	-61.66	-51.65	-47.59	-40.81	-31.72	-26.76	-46.31	-50.32	-57.72
b1_4	-51.89	-41.39	-55.46	-33.35	-49.65	-37.68	-51.55	-55.67	-64.55
b1_5	-47	-44.49	-33.64	-20.86	-28.01	-14.65	-39.44	-32.34	-54.38
Data after normalization									
Healthy	-46.85	-48.01	-47.96	-48.31	-37.46	**0**	-46	-49.74	-47.68
b1	-40.68	-43.12	-21.93	-16.17	-11.94	**0**	-35.74	-25.48	-37.37
b1_2	-38.48	-32.39	-18.06	-8.89	-3.73	**0**	-19.24	-33.22	-34.23
b1_3	-34.9	-24.89	-20.83	-14.05	-4.96	**0**	-19.55	-23.56	-30.96
b1_4	-14.21	-3.71	-17.78	4.33	-11.97	**0**	-13.87	-17.99	-26.87
b1_5	-32.35	-29.84	-18.99	-6.21	-13.36	**0**	-24.79	-17.69	-39.73

interaction between the $3f_s$ stator magnetic field and the broken bar fault related $\pm 3sf_s$ rotor magnetic field. The two signatures located to the right of the $6f_s$ are related to the speed ripple effect. In our case the speed ripple effect is very important because it is directly related to the relative position of the broken rotor bars. The resulting indicator is shown in Fig. 5. It is clear that the fault severity level is now evident.

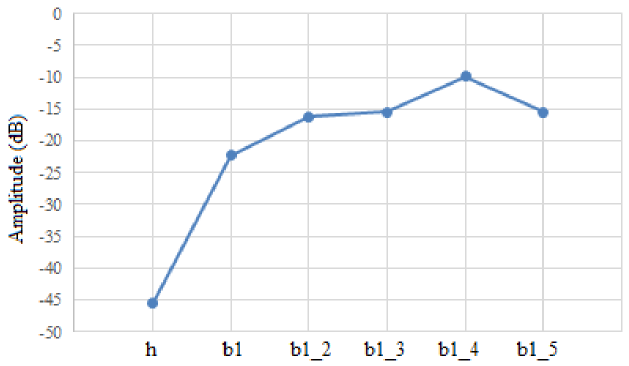

Fig. 5. The amplitude of the proposed fault indicator for all studied cases.

IV. Conclusions

In this work, a new procedure has been adopted and presented aiming to the reliable detection of non-adjacent broken rotor bars. The new approach has three stages. In the first stage the application of the FPVA can lead to a fast diagnostic alarm regarding the fault's existence. Then the FEPVA is applied which consists of the analysis of the filtered Park's vector modulus spectrum. Finally, a new indicator is calculated using specific signatures' amplitudes occuring from the FEPVA. It has been shown that this indicator is able to discriminate with reliability and accuracy the different faulty conditions and adjust the fault level severity independently from the broken bars relative position.

V. References

[1] W. T. Thomson, M. Fenger, "Current signature analysis to detect induction motor faults" *IEEE Industry Applications Magazine*, July/August 2001, pp. 26-34.

[2] D. B. Durocher, G. R. Feldmeier,"Predictive versus preventive maintenance", *IEEE Industry Applications Magazine*, Vol. 10, No.5, October 2004, pp. 12-21.

[3] S. B. Lee, E. Wiedenbrug., K. Younsi, "ECCE 2013 Tutorial: Testing and Diagnostics of Induction Machines in an Industrial Environment", Denver, CO, USA, Sep 2013.

[4] T-J. Yang, D. Kang, Hyun, S. B. Lee, J. A. Antonino-Daviu, J. Pons-Llinares, "Reliable Detection of Induction Motor Rotor Faults Under the Rotor Axial Air Duct Influence," *IEEE Trans. Ind. Appl*., vol. 50, no. 4, pp. 2493-2502, Jul.-Aug. 2014.

[5] J. A. Antonino Daviu, J. Pons-Llinares, and S. B. Lee, "Advanced Rotor Fault Assessment for High Voltage Induction Motors via Continuous Transforms," *Proc. of PCIC Europe*, pp. 57-63, June 2015.

[6] A. Bellini, et al., "On-field experience with on-line diagnosis of large induction motors cage failures using MCSA," *IEEE Trans. on Ind. Appl.*, pp. 1045-1053, vol. 38, no. 4, July/Aug. 2002.

[7] I. M. Culbert, and W. Rhodes, "Using current signature analysis technology to reliably detect cage winding defects in squirrel-cage induction motors," *IEEE Trans. on Ind. Appl.*, vol. 43, no.2, pp.422-428, Mar./Apr. 2007.

[8] R. R. Schoen and T. G. Habetler. "Evaluation and Implementation of a System to Eliminate Arbitrary Load Effects in Current-Based Monitoring of Induction Machines," *IEEE Trans. Ind. Appl.*, vol.33, no. 6, pp. 1571-1577, November/December 1997.

[9] J. A. Antonino-Daviu, M. Riera-Guasp, J. R. Folch, and M. Pilar Molina Palomares, "Validation of a new method for the diagnosis of rotor bar failures via wavelet transform in industrial induction machines," *IEEE Trans. Ind. Appl.*, vol. 42, pp. 990-996, 2006.

[10] S. Shin, J. Kim, S. B. Lee, and C. Lim, "Evaluation of the Influence of Rotor Magnetic Anisotropy on Condition Monitoring of 2 Pole Induction Motors," *Proc. of IEEE ECCE*, Sept. 2014.

[11] J. A. Antonino-Daviu, M. Riera-Guasp, J. Pons-Llinares, J. Park, S. B. Lee, J. Yoo and C. Kral, "Detection of Broken Outer Cage Bars for Double Cage Induction Motors under the Startup Transient", *IEEE Transactions on Industry Applications*, vol. 48, no.5, pp. 1539-1548, Sept-Oct. 2012.

[12] M. Drif and A. J. M. Cardoso, "Discriminating the Simultaneous Occurrence of Three-Phase Induction Motor Rotor Faults and Mechanical Load Oscillations by the Instantaneous Active and Reactive Power Media Signature Analyses," *IEEE Trans. Ind. Elec*., Vol. 59, No. 3, pp. 1630-1639, 2012.

[13] J. Kim, S. Shin, S. B. Lee, K. N. Gyftakis, M. Drif and A. J. M. Cardoso, "Power spectrum-based detection of induction motor rotor faults for immunity to false alarms," *IEEE Trans. Ener. Conv.*, vol. 30, Nº 3, pp.1123-1132, September 2015.

[14] M. Sahraoui, A. J. M. Cardoso, A. Ghoggal, "The use of a modified Prony method to track the broken rotor bars characteristic frequencies and amplitudes, in three-phase induction motors", *IEEE Trans. Ind. Appl*., vol. 51, No. 3, pp. 2136-2147, May/June 2015.

[15] J. Park, B. Kim, J. Yang, K. Lee, S. B. Lee, E. J. Wiedenbrug, M. Teska, and S. Han, "Evaluation of the Detectability of Broken Rotor Bars for Double Squirrel Cage Rotor Induction Motors," *in proc. of the IEEE ECCE*, pp. 2493-2500, Sept. 2010.

[16] M. Riera-Guasp, M. Fernández Cabanas, J. Antonino-Daviu, M. Pineda-Sánchez, C. H. Rojas, "Influence of not-Consecutive Bar Breakages in Motor Current Signature Analysis for the Diagnosis of Rotor Faults in Induction Motors", *IEEE Transactions on Energy Conversion*, vol.25, no.1, pp.80-89, March 2010.

[17] C. Hargis, B. G. Gaydon, and K. Kamash, "The detection of rotor defects in induction motors," *Proc. 1982 IEE Int. Conf. Electr. Mach., Des. Appl.*, London, U.K., pp. 216–220.

[18] M. Benbouzid, "A review of induction motors signature analysis as a medium for faults detection," *IEEE Trans. Ind. Electron*., vol. 47, no. 5, pp. 984–993, Oct. 2000.

[19] T. J. Sobczyk and W. Maciolek, "Does the component (1-2s)f0 in stator current is sufficient for detection of rotor cage faults?," Proc. Int. Symp. Diagnostic Elect. Mach., Power Electron. Drives (SDEMPED 2005), Vienna, Austria, Sep. 2005.

[20] A. Menacer, S. Moreau, G. Champenois, M. S. N. Said, A. Benakcha, "Experimental detection of rotor failures of induction machines by stator current spectrum analysis in function of the broken rotor bars position and the load," Proc. Int. Conf. Comput. Tool, Sep. 2007, pp. 1752–1758.

[21] J. Faiz B. M. Ebrahimi, "Locating rotor broken bars in induction motors using finite element method," Energy Convers. Managem., vol. 50, no. 1, pp. 125–131, Jan. 2009.

[22] G. Y. Sizov, A. Sayed-Ahmed, Y. Chia-Chou, N. A. O. Demerdash, "Analysis and diagnostics of adjacent and nonadjacent broken rotor bar faults in squirrel-cage induction machines," IEEE Trans. Ind. Elec.., vol 56, no. 11, pp. 4627–4641, Nov. 2009.

[23] M. Riera-Guasp, J. Pons-Llinares, F. Vedreno-Santos, J. A. Antonino-Daviu, M. F. Cabanas, "Evaluation of the amplitudes of high-order fault related components in double bar faults," *Proc. of the 8th IEEE International Symposium on Diagnostics for Electric Machines, Power Electronics and Drives, SDEMPED 2011*, Bologna, Italy, September 2011.

[24] A. J. M. Cardoso, E. S. Saraiva, "On-line diagnostics of three-phase induction motors, by Park's vector," *Proc. of the International Conference on Electrical Machines*, Pisa, Italy, Vol. III, pp. 231-234, September 12-14, 1988.

[25] S. M. A. Cruz, A. J. M. Cardoso, "Rotor cage fault diagnosis in three-phase induction motors, by Extended Park's Vector Approach," *Electric Machines and Power Systems,* Vol. 28, No. 4, pp.289-299, April 2000.

[26] A. J. M. Cardoso, S. M. A. Cruz, J. F. S. Carvalho and E. S. Saraiva, "Rotor Cage Fault Diagnosis in Three-Phase Induction Motors, by Park's Vector Approach," *Conference Record of the Thirtieth IAS Annual Meeting, IAS '95*, Vol. 1, pp. 642-646, Orlando, FL, Oct. 1995.

[27] F. Filippetti, G. Franceschini, C. Tassoni and P. Vas, “AI techniques in induction machines diagnosis including the speed ripple effect”, *IEEE Trans. Ind. Appl*., Vol. 34, No. 1, pp. 98-108, 1998.
[28] H. Henao, H. Razik, and G.-A. Capolino, “Analytical approach of the stator current frequency harmonics computation for detection of induction machine rotor faults,” *IEEE Trans. Ind. Appl.*, vol. 41, no. 3, pp. 801–807, May/Jun. 2005.
[29] J. Cusido, J. Rosero, and E. Aldabas, “New fault detection techniques for induction motors,” *Electr. Power Quality Utilisation, Mag.*, vol. II, no. 1, pp. 39–46, 2006.

VI. Biographies

Konstantinos N. Gyftakis (M'11**)** was born in Patras, Greece, in May 1984. He received the Diploma in Electrical and Computer Engineering from the University of Patras, Patras, Greece in 2010. He pursued a Ph.D in the same institution in the area of electrical machines condition monitoring and fault diagnosis (2010-2014). Then he worked as a Post-Doctoral Research Assistant in the Dept. of Engineering Science, University of Oxford, UK (2015). He is currently a Lecturer, School of Computing, Electronics and Mathematics, Faculty of Engineering, Environment and Computing and an associate with the Research Centre for Mobility and Transport, Coventry University, UK. His research activities are in fault diagnosis, condition monitoring and degradation of electrical machines. He has authored/co-authored more than 35 papers in international scientific journals and conferences. (E-mail: k.n.gyftakis@ieee.org).

Jose A. Antonino-Daviu (S'04/M'08/SM'12) received his M.S. and Ph. D. degrees in Electrical Engineering, both from the Universitat Politècnica de València, in 2000 and 2006, respectively. He was working for IBM during 2 years, being involved in several international projects. Currently, he is Associate Professor in the Department of Electrical Engineering of the mentioned University, where he develops his docent and research work. He has been invited professor in Helsinki University of Technology (Finland) in 2005 and 2007, Michigan State University (USA) in 2010 and Korea University (Korea) in 2014. He has over 100 publications between international journals, conferences and books. His primary research interests are condition monitoring of electric machines, wavelet theory and its application to fault diagnosis and design and optimization of electrical installations and systems.

Antonio J. Marques Cardoso (S'89, A'95, SM'99) received the Dipl. Eng., Dr. Eng., and Habilitation degrees from the University of Coimbra, Coimbra, Portugal, in 1985, 1995 and 2008, respectively, all in Electrical Engineering. From 1985 until 2011 he was with the University of Coimbra, Coimbra, Portugal, where he was Director of the Electrical Machines Laboratory. Since 2011 he has been with the University of Beira Interior (UBI), Covilhã, Portugal, where he is a Full Professor at the Department of Electromechanical Engineering and Director of CISE - Electromechatronic Systems Research Centre (http://cise.ubi.pt). He was Vice-Rector of UBI (2013-2014). His current research interests are in fault diagnosis and fault tolerance in electrical machines, power electronics and drives. He is the author of a book entitled Fault Diagnosis in Three-Phase Induction Motors (Coimbra, Portugal: Coimbra Editora, 1991), (in Portuguese) and more than 350 papers published in technical journals and conference proceedings. He serves as Guest Editor of the *IEEE Transactions on Industry Applications* Special Issue on *Fault Diagnosis of Electric Machines, Power Electronics and Drives* and Associate Editor for the *IEEE Transactions on Industry Applications*, *IEEE Transactions on Industrial Electronics*, *IEEE Journal of Emerging and Selected Topics in Power Electronics*, and also for the Springer *International Journal of Systems Assurance Engineering and Management*.